The Investigation of the Influence of Back Contact Metal and Ligand Exchanging on the Air Stability of Ambient Processed Schottky Photovoltaic Cells Based on PbSe CQDs

**M. SHISHEHBORI[1], A. A. ABDOLHOSSEINZADEH[2]*,
M. R. SEYEDMIR[3] and M. ABDOLHOSSEINZADEH[4]**

(Received: January 20, 2012; Accepted: March 04, 2012)

[1]Islamic Azad University, Yazd Branch, Physics Department, Yazd 8916871967, Iran.
[2]Nano Gostare Kavire Yazd Co., Science and Technology Park, Yazd 8916871967, Iran.
[3]Islamic Azad University, Yazd Branch, Scientific Society of Nanotechnology, Yazd 8916871967, Iran.
[4]Islamic Azad University, Taft Branch, Physics Department, Yazd 8916871967, Iran.
*Corresponding author: E-mail: aaa6284@gmail.com

ABSTRACT

In this work we fabricated and tested nanocrystalline schottky solar cells based on PbSe CQDs. Crystalline and monodisperse PbSe capped oleic acid CQDs were synthesized through hot injection reaction. From absorption peak and narrow photoluminescence peak of QDs in solution, CQDs size (~3 nm) and monodispersity of CQDs were determined. Photovoltaic cell structure is formed from PbSe QDs sandwiched between Al (or Ag) and ITO electrodes as electron and hole transporter layers, respectively. Current-Voltage characteristics showed carrier separation mechanism consistent with schottky device structure. The best efficient cell obtained, without any nanocrystalline film thickness optimization, with ITO\PbSe QDs\LiF\Al structure showed a PCE of 0.55%. Furthermore, oleylamine based devices with Ag as back contact exhibited the most durable cells with the life time of 21 h and survival until 5 days.

Keywords: PbSe CQDs, Schottky Cells, Ligand Exchange, Nanocrystalline Photovoltaics

INTRODUCTION

During the past decade, nanomaterials, nanostructures and their applications have been widely investigated.[1-12] Also, enormous research has been done on nanoparticles[6], nanowires[7-9] and nanocomposites[10-11] to develop low-temperature processed photovoltaic (PV) cells. Because of the possibility of solution processing, colloidal quantum dots (CQDs) are appropriate for large area, low cost solar cells. CQDs based solar cells have already achieved 5.1% solar power conversion efficiency (PCE). [13]

Among the CQD materials, lead sulfide (PbS) and lead selenide (PbSe) CQDs have been the focus of research efforts, because of their

optimal band gap and excellent photosensitivity.[14-17] Also, because of the low energy band gaps, they are able to absorb larger portions of solar power in the infrared region.[18-19] Different solar cell structures including schottkies and p-n junctions have been fabricated and tested.[18-20]

Schottky cells based on PbSe CQDs have reached PCE of 3.3%, but in all reports, devices have been found to suffer a major limitation: a lack of air stability.[15] Fabrication and characterization procedures must be performed in an inert environment. so that, butylamine capped PbS CQDs degraded within minutes of exposing to air.[21] Later, Luther et al.[17] described a schottky barrier photovoltaic cell consisting of oleic acid capped PbSe nanocrystals (NCs) that produced an exceptionally large short-circuit (I_{sc}) photocurrent (>21 mA/Cm^2) reaching 2.1% of PCE. They treated nanocrystalline film with ethanedithiol (EDT) to remove the electrically insulating oleate ligands. But these devices also degraded rapidly in air.

Passivating PbSe CQDs with 1,4-Benzenedithiol produced devices stable in air over a few hours.[19] Tang et al. [22] posited two areas of possible degradation: 1) within the nanocrystalline film: labile ligands make the film particularly vulnerable to attack by oxygen and moisture 2) at the semiconductor-metal interface: shallow work function metals are known to be oxidized rapidly or react with ligands in the film. They developed oleylamine exchanged PbS CQDs based schottky PV cells stable in air over days, a significant improvement.[22] achieving for such stabilities seems to be difficult in the case of PbSe CQDs so far because PbSe CQDs are more reactive than PbS against air and moisture.

In this study we combine 5 strategies reported for improving air stability of schottky photovoltaic cells based on different CQDs, apply them to PbSe CQDs and represent photovoltaic devices based on PbSe CQDs, stable in air for days. We also investigate the influence of different parameters such as ligand exchanger and back contact types on device performance and stability.

EXPERIMENTAL

Materials

Oleic acid (OA, technical grade 90%), 1-octadecene (ODE, technical grade 90%), Trioctylphosphine (TOP, technical grade, 90%), diphenylphosphine (DPP, 98%) and selenium powder (Se, 97% purity) were purchased from Sigma-Aldrich and Lead(II) oxide powder (PbO, 99%) was purchased from Merck. 1,2-ethanedithiol (EDT, 97%) was acquired from Fluka. Acetone, ethanol and hexane were purchased from Merck.

CQDs Synthesis

Standard air free hot injection method was used for synthesizing of monodisperse oleate capped PbSe CQDs in a three neck 50 cc flask. The mixture of 500 mgr of PbO and 1.6 cc of OA were dissolved in 11.5 cc of ODE under vigorous stirring while the mixture being heated under N_2 flow for 1 hour until a clear solution appeared. Then, 550 mgr of Se, 0.03 cc of DPP and 6 cc of TOP were added into the Pb oleate solution. After 90 seconds, the solution was cooled down with a cold water bath. After the synthesis was completed, The PbSe CQDs precipitation was carried out using acetone and ethanol-hexane. Then, CQDs were dried and stored as powder.

Ligand Exchange

The ligand exchange process was performed inside an argon-filled glove box. 1 cc of octylamine was injected to redisperse PbSe CQDs powder and the solution was stored for 3 days. After that, the CQDs were precipitated again by ethanol and were redispersed in hexane to yield 35 mg/ml stock solution. This process also repeated for butylamine and oleylamine ligand exchanged PbSe CQDs.

Device Fabrication

All device fabrication occurred in ambient atmosphere using a layer-by-layer spin coating technique. A solution of 0.01 M of EDT in acetonitrile was prepared in advance. Ligand exchanged PbSe CQDs in hexane were spin coated on a clean and etched Glass\ITO (20 ohm/Sq, 300 nm) substrate followed by EDT treatment. 3 cycles were used to make the films with desired thickness. All spin

coating cycles were at 1500 rpm, for 60s with maximum acceleration rate. After 10 minutes thermal annealing of the film at 110Úc in air, top contacts were deposited through a shadow mask in a thermal evaporator. The Al, Ag and LiF/Al electrodes thicknesses were 70nm, 100nm and 0.8nm/70nm, respectively.

Characterization

Room temperature UV-Vis-NIR absorption and PL emission spectrometries were conducted using diluted colloidal solutions of nanoparticles. UV-Vis-NIR absorption spectra were recorded on a LAMBDA 950 UV-Vis-NIR Spectrophotometer. PL measurements were taken on a Perkin-Elmer LS-55 Spectro-photometer and all the samples were excited at 235 nm under same conditions. All current-voltage measurements were taken with Ivium Stat Electrochemical Interface & Impedance Analyzer. A SolSim: Luzchem solar simulator based on a powerful 300W ceramic xenon lamp, operating at 100 mW/Cm^2 was used to simulate the solar spectrum under AM1.5G conditions.

RESULTS AND DISCUSSION

As shown in Fig. 1 a, as-synthesized PbSe CQDs dispersed in hexane exhibit a well-defined first excitonic absorption peak centered at 1050 nm. The full width at half maximum (FWHM) of this first excitonic transition peak is around 100 nm. The average particles size is determined using the formula proposed by Iwan Morels et al.[23] Considering that the band gap (E0) can be determined very precisely from absorbance measurements, using the size obtained from this equation is more accurate than using the size from TEM measurements (valid in the range 2–20 nm):

$$E_o = 0.278 + \frac{1}{0.016d^2 + 0.209d + 0.45}$$

Where E_0 is the band gap in unit of eV and d is the mean particle diameter (nm). Substituting 1.18 eV for E_0, yields the average particle size of our PbSe CQDs approximately 3 nm.
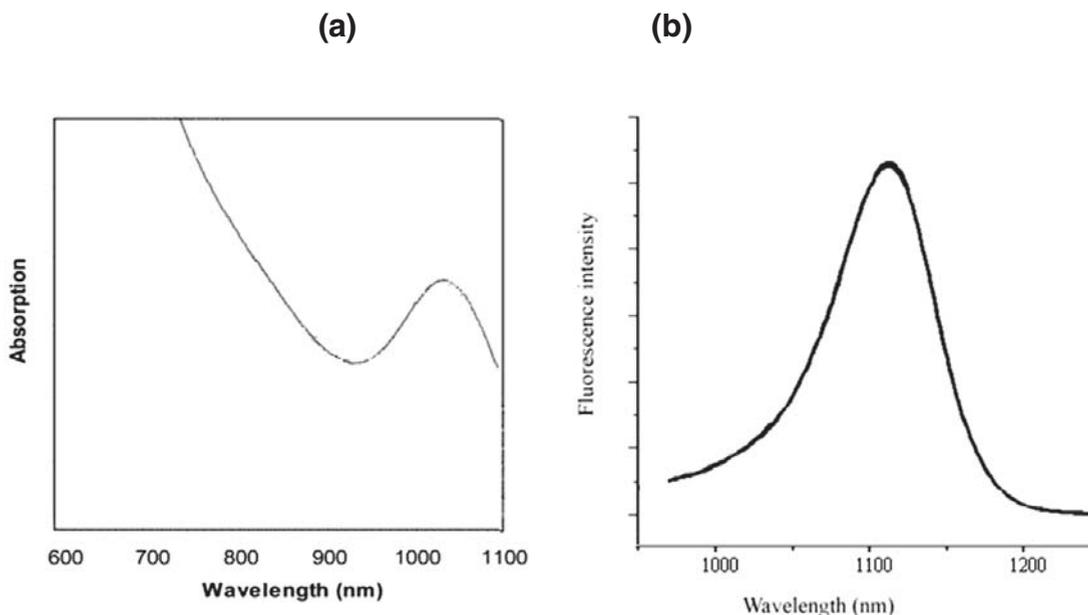
(a)   **(b)**

Fig. 1. a) absorption and b) emission spectra of 3 nm in diameter oleic acid capped PbSe CQDs in solution used for device fabrication. The spectra were recorded using colloidal QDs solution in hexane.

The PL spectrum of PbSe CQDs is shown in Fig. 1 b. The FWHM of CQDs emission peak is around 100 nm. Narrow PL peak indicates narrow size distribution and monodispersity of PbSe quantum dots in suspension. Stokes shift (difference in wavelength between excitonic absorption peak and emission peak) is 70 nm. As shown in Fig. 2 b, PbSe CQDs with ~3 nm in diameter produced by hot injection method show an emission peak at 1120 nm.

To investigate the reproductivity of the synthesis method discussed here, several CQDs samples were synthesized. Standard deviation in the position of excitonic absorption peak was less than 13 nm.

Based on all material characterization procedures applied herein, extremely small, high quality and reproducible PbSe CQDs can be obtained using this chemical hot injection method. As-synthesized CQDs are approximately 3 nm in size, monocrystalline and lead reach with optical absorption centered at 1050 nm.

In our photovoltaic cell preparation strategy, CQDs synthesis and ligand exchange were occurred under inert gas. While, CQDs precipitation, centrifugation and drying, deposition of CQDs as thin films and characterization of solar cells were carried out under ambient. Also, we used ordinary acetone, hexane and ethanol solutions for washing and precipitation of CQDs rather than their anhydrous solutions. Although this process (preparation in ambient and using ordinary solutions) reduces final cell PCE, but has substantial influence on fabricating devices more easily and quickly, reducing fabrication costs and enhancing device durability.

We combined five techniques for improving the performance and air stability of nanocrystalline based photovoltaic cells and applied them to schottky cells based on PbSe CQDs and specifically concentrated on enhancing air stability of these devices. These techniques were: 1) using smaller QDs sizes (3 nm in diameter), 2) ligand exchange (octylamine and oleylamine in this case), 3) using more stable back contact metals than Al such as Ag and sandwiching an passive intermediate layer between NCs layer and back contact, 4) thermal annealing and 5) chemical treatment. This strategy was applied to all devices without further optimization, for example, in CQDs synthesis, NCs array and electrodes thickness and so on.

Solar cells fabricated from ligand exchanged PbSe CQDs, treatments applied on nanocrystalline film and back contact types are tabulated in table 1.

Long oleic acid ligands (2.5 nm) on as-synthesized CQDs are first exchanged by other - amine ligands, which are replaced in the next by EDT ligands through another ligand exchange process. ligand exchange of insulating oleic acid ligands with smaller octylamine ones help close packing of CQDs in the nanocrystalline array and consequently, improves electrical transport properties among neighboring CQDs.[24] This process also, improves film resistance to oxidation against moisture and air of ambient storage and CQDs surface passivation continues for longer times[22]. So that, any photovoltaic performance were observed from photovoltaic cells fabricated by deposition of only-oleic acid capped CQDs.

A layer by layer spin coating strategy was applied for deposition of ligand exchanged PbSe

Table 1: Summary of fabrication processes for five representative photovoltaic cells

	Ligand exchange	Thermal annealing	Chemical treatment	Back contact
1	octylamine	110°C, 10 minutes	EDT	Al
2	octylamine	110°C, 10 minutes	EDT	Ag
3	octylamine	110°C, 10 minutes	EDT	LiF/Al
4	oleylamine	110°C, 10 minutes	EDT	Ag
5	butylamine	110°C, 10 minutes	EDT	Ag

Table 2: Dependence of cell properties on the type of the back contact layer for octylamine and oleylamine ligand exchanged PbSe CQDs based schottkies processed under same thermal and chemical treatments.

	V_{oc}(V)	I_{sc}(mA/Cm²)	FF (%)	PCE (%)
1	0.2	3.25	57	0.37
2	0.13	2.4	41	0.13
3	0.32	3.18	53	0.55
4	0.18	2.6	45	0.21

CQDs, such that any pinholes from the EDT treatment were filled in using the next layer. This layer by layer process, helps creating of uniform nanocrystalline film without any pinhole or crack. Whole nanocrystalline array deposition is formed by three cycles of CQDs coating and EDT treatment. On the other hand, EDT chemical treatment of nanocrystalline film after CQDs deposition, lead to improvement of electronical transport properties and reduction of nanocrystalline film solubility. Furthermore, thermal annealing in air done at 110°C for 10 minutes, lead to some preoxidation of CQDs prior to metal contact deposition and improvement in schottky cell stability. [22, 25]

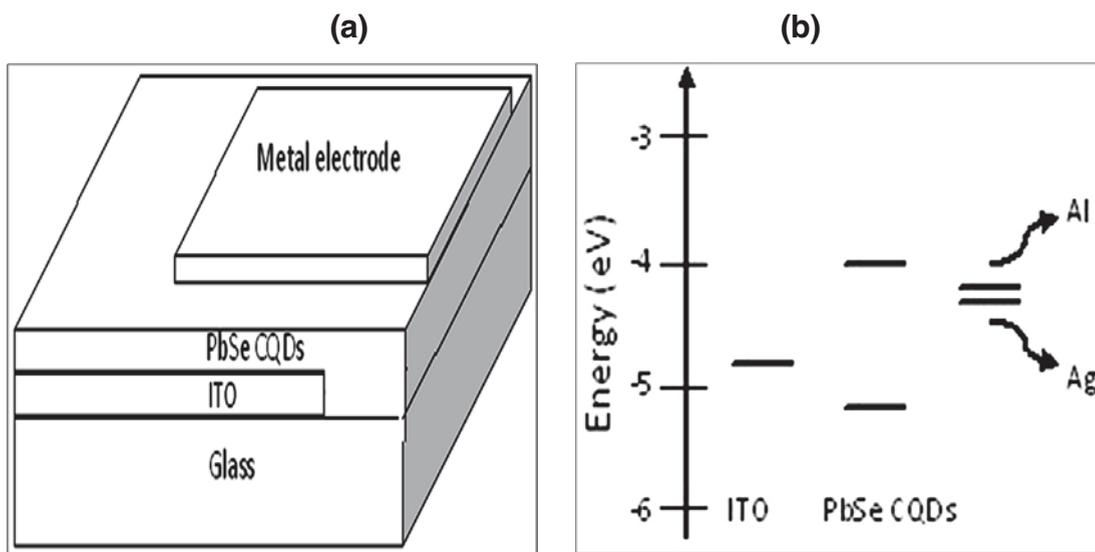**(a)**   **(b)**

Fig. 2. a) Schematic structural image and b) energy levels (metal work functions and PbSe QDs HOMO-LUMO level) diagram of our 3 nm in diameter PbSe CQDs based schottky photovoltaic cells. Al electrode produced larger V$_{oc}$, while Ag electrode yielded more stable devices.

Because Ag is less reactive than Al, [26] and its reaction with exchanging ligands is much lesser, it can reduce decay of the schottky contact in air. This selection led to formation of photo- and air-stable cells with AM1.5G PCE of 0.13% under illumination.

Schematic image of our cell along with proposed energy levels diagram is shown in Fig. 2. this diagram was drawn based on prior reports about determining the band alignment of various CQDs sizes using absorption spectroscopy and cyclic voltametry.[16] Based on this work, 4 eV and 5.2 eV for valence and conduction band edges of PbSe quantum confined CQDs with 3 nm in size is approximated.[16, 22]

In attention to P-type dopping of EDT treated PbSe CQDs and shallow work functions of Al (ø=4.2 eV) and Ag (ø=4.3 eV), a schottky barrier is formed at the semiconductor-metal junction which lead to band bending and depletion region (Fig. 3). ITO (ø=4.8 eV) establishes an ohmic contact with p-type PbSe layer. Under illumination,

electron-hole pairs inside depletion region are separated by built-in electrical field and electrons transport to Al or Ag electrode and holes to ITO electrode (Fig. 3).

The current-voltage and PV performance of devices under illumination (AM1.5G, 100 mW/Cm^2) are shown in Fig. 4 and key device parameters extracted are listed in table 2. For ITO\PbSe QDs\Al device, V_{oc}, I_{sc} and FF are 0.2, 3.25 and 57% respectively, exhibiting 0.37% power conversion efficiency. But the device degraded in air within several hours because of the reaction of Al with ligands (on the surface of CQDs) in the film. If we define the life time as the duration of the cell survival to 80% of its initial PCE, the life time of Al based device was under 40 minutes (Fig. 5 a). Previous works reported devices without thermal annealing and ligand exchange processes working for weeks inside a glove-box while minute's removal of devices led to rapid degradation.[15,16] Strikingly, octylamine and oleylamine processed CQDs based solar cells showed improved air stability in ambient storage.

By the same criterion, For ITO\PbSe QDs\Ag devices, V_{oc}, I_{sc} and FF are 0.13, 2.4 and 41%, showing 0.13% of PCE, which is 60% less than the device based on Al metal electrode, while its life time was 15 h and its survival was above 3 day, a 24-fold increase in longevity compared to Al based device (Fig. 5 c).

To combine higher efficiency of Al electrode with longer stability of Ag electrode, we sandwiched a thin (0.8 nm) LiF layer between nanocrystalline layer and Al metal contact. This layer eliminates reaction between Al and organic ligands, leading to higher durability and performance. So that, the devices with ITO\PbSe QDs\LiF\Al structure showed a PCE of 0.55%, a 1.5-fold improvement compared with pure Al based devices. Furthermore, its life time is 6 h (Fig. 5 b). So, one area of device degradation is at the metal-nanocrystalline array interface and its rate depends on the metal contact type. The metal contacts can react with QDs ligands or may be oxidized themselves. Both Al and Ag metals can produce schottky junction with PbSe nanocrystalline array leading to air stable devices. Devices based on pure Ag have the most stability. Introducing LiF layer improves stability (1.5-fold) and performance
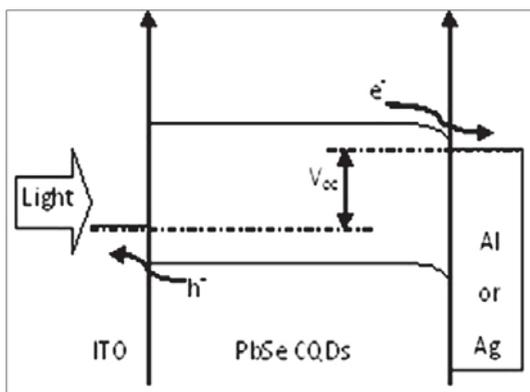

Fig. 3. Band diagram of our ITO/NCs film/metal device. Extracted open circuit voltage (V$_{oc}$) is the energy difference between ITO and Al work functions. Band bending occurs at the NCs/metal contact interface and electrons flow to the back contact electrode.
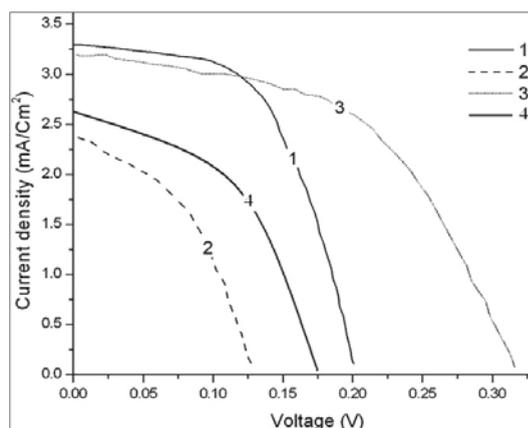

Fig. 4: Current voltage characteristics of samples 1, 2,3 and 4 under AM 1.5 G, 100 mW/Cm^2 illumination (device active area of 0.09 Cm^2). Devices were characterized under ambient and tests were performed regularly until stability life times were obtained under one son conditions for schottky devices based on PbSe CQDs having a band gap of 1.18 eV (1050 nm first excitonic peak)

(~ 9-fold) compared with pure Al based devices, But its durability is much less than Ag based devices. LiF layer modifies schottky interface and improves V_{oc} and I_{sc} and consequently improves efficiency.

We further generalized our combined strategy to butylamine (0.5 nm) and oleylamine (2.5 nm) as ligand exchanger to investigate the role of different ligands on the performance and durability of photovoltaic cells. The devices were fabricated using ITO\PbSe QDs\Ag structure and chemical and thermal treatments were conducted like the device labeled 3 in table 1 based on octylamine ligand exchanged PbSe QDs. Devices made from butylamine ligand showed no photovoltaic

performance, although showing diode characteristic in their I-V curve which can be attributed to the 2 properties of butylamine ligands: 1) more Reactivity with shallow-work-function metal back contacts and 2) butylamine ligands are too short to create a strong protective layer around CQDs against air and moisture of the environment. Although short ligands such as butylamine are consistent with inter-nanocrystalline carrier transport, but cannot tolerate the passivation of nanocrystals surfaces in ambient environment. So, the selection of ligands with stronger binding end groups is inevitable.

To achieve longer stabilities, oleylamine ligand exchanged PbSe CQDs based devices with
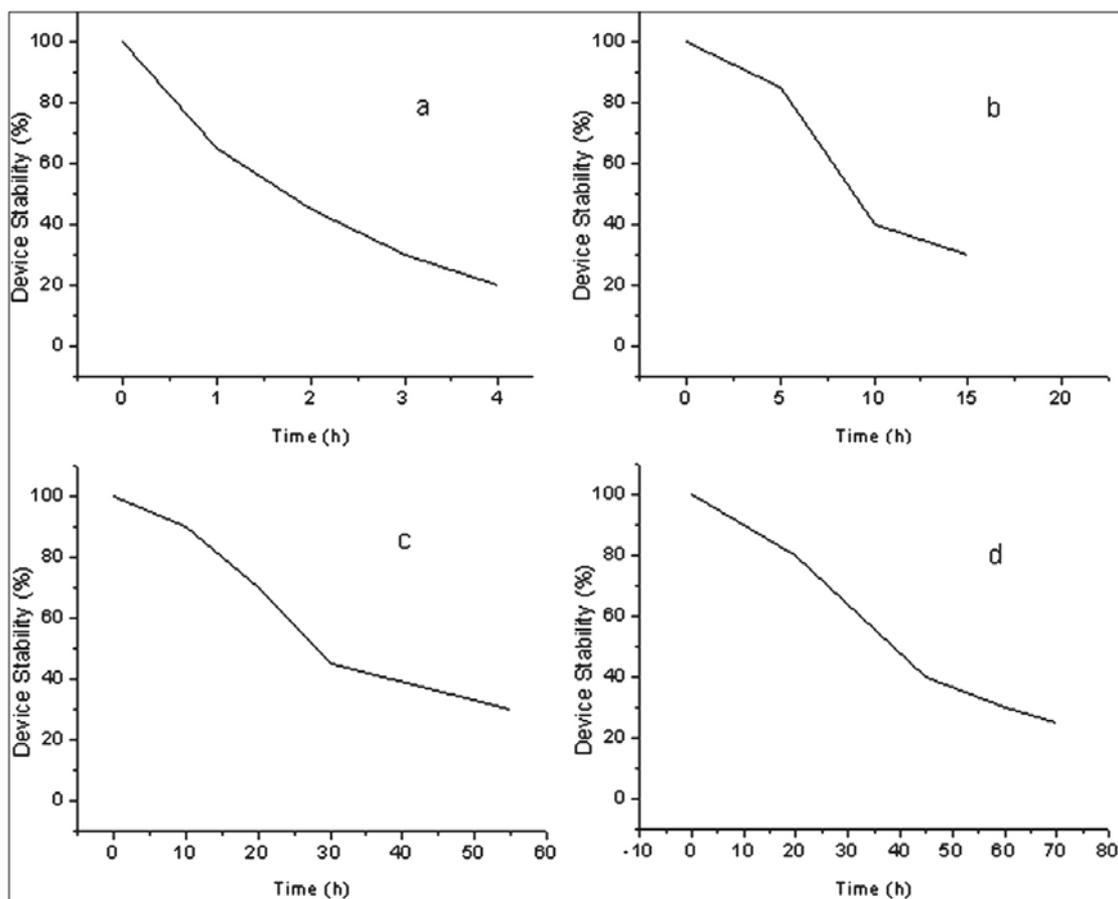

Fig 5. The evolution of device performance (PCE) in time for devices fabricated and stored in air. a) Octylamine based device with Al as back contact, b) octylamine based device with Ag as back contact, c) octylamine based device with LiF/Al as back contact and d) oleylamine based device with Ag as back contact. The PCE values were taken under 100 mW/Cm².

ITO\PbSe QDs\Ag structure were fabricated and enhanced performance and stability with regard to octylamine ligand exchanged based devices obtained. Strikingly, devices using oleylamine showed significant stability: their life time was 21 h and their performance extends beyond 5 days. These devices also, showed improved PCE compared with octylamine based devices (Fig. 5 d). Oleylamine is a long-chain ligand, similar to oleic acid, but less strongly-bound. It seems that oleylamine capping ligands expose nanocrystalline-film to pre-oxidation, to some extent, which leads to higher device I_{sc} While, shorter butylamine and octylamine ligands make nanocrystalline-film vulnerable for unwanted oxidation. Although the most part of exchanging ligands remove from nanocrystalline film during chemical treatment and thermal annealing, but their role in making denser films and a protecting layer around CQDs against oxidation during film formation provides improved air stability in ambient storage.

Devices fabricated in an inert environment without intermediate solution-phase ligand exchange process exhibited initial improvement in their I_{sc} and FF, leading to improvement in PCE during the first minutes after air exposure. Then, their performance instantly decreased. The increase in the I_{sc} is likely due to an increase in the conductivity of the PbS film upon oxygen exposure or a decrease in the device resistance that may result from repetitive electrical measurement. But as we can see in Fig. 5 d, our unpackaged, stable devices fabricated entirely in ambient through our strategy, showed almost constant and gradual degradation, and retained part of their performance even after 5 days.

CONCLUSION

We fabricated PbSe CQDs based schottky solar cells. Small ~3 nm monodispersed PbSe CQDs were synthesized by chemical hot injection method which had band gap of 1.18 eV. Photoluminescence spectra revealed narrow emission with full width at half maximum of 100 nm at 1120 nm. By applying thermal treatment, ligand exchange and chemical treatment with a dithiol, we modified CQDs surface properties in nanocrystalline array and consequently, improved photovoltaic cell performance and durability. By incorporation of a thin layer of LiF between nanocrystalline layer and Al electrode, photovoltaic performance, photo- and air-stability of the cell significantly improved. More stable devices obtained by the combination of oleylamine as a ligand exchanger and Ag as a metal electrode, surviving for more than 5 days.

ACKNOWLEDGMENTS

REFERENCES

1. C. B. Murray, D. J. Norris, M. G. Bawendi, *Am. Chem. Soc.* **115** , 8706 (1993).
2. M. H. Yousefi, A. A. Abdolhosseinzadeh, H. R. Fallah and A. A. Khosravi, *Mod. Phys. Lett. B*, **24** , 2591 (2010).
3. C. N. R. Rao and A. K. Cheetham, *J. Mater. Chem.* **11**, 2887 (2001).
4. M. Grundmann, *Nano-optoelectronics: concepts, physics, and devices* (Springer) (2002).
5. D. M. M. Atwa, I. M. Azzouz and Y. Badr, *Appl. Phys. B,* **79** , 673 (2004).
6. W. Hillhouse and M. C. Beard, *Curr. Opin. Colloid Interface Sci.* **14** , 245 (2009).
7. A. Kandala1, T. Betti and A. F. Morral, *phys. status solidi A*, **206** , 173 (2009).
8. J. Jie, W. Zhang, I. Bello, C. S. Lee and S. T. Lee, *Nano Today*, **5** , 313 (2010).
9. Y. N. Xia, , P. D. Yang, Y. G. Sun, Y.Y. Wu, B. Mayers, B. Gates, Y. D. Yin, F. Kim and Y.Q. Yan, *Adv. Mater.* **15** , 353 (2003).
10. H. Tributsch, *J. Solid State Electrochem.* **13** , 1127 (2009).
11. M. Nanu, J. Schoonman and A. Goossens, *Adv. Maert.* **16** , 453 (2004).
12. D. V. Talapin, J. S. Lee, M. V. Kovalenko and E.

V. Shevchenko, *Chem. Rev.* **110,** 389 (2010).

13. A. G. Pattantyus-Abraham, I. J. Kramer, A. R. Barkhouse, X. Wang, G. Konstantatos, R. Debnath, L. Levina, I. Raabe, M. K. Nazeeruddin, M. Gratzel and E. H. Sargent, *ACS Nano* **4** , 3374 (2010).

14. R. Dalven, *Infrared Phys.* **9** , 141 (1969).

15. W. Ma, J. M. Luther, H. Zheng, Y. Wu and A. P. Alivisatos, *Nano Letts.* **9** , 1699 (2009).

16. J. J. Choi, Y. F. Lim, M. B. Santiago-Berrios, M. Oh, B. R. Hyun, L. Sun, A. C. Bartnik, A. Goedhart, G. G. Malliaras, H. D. Abruna, F. W. Wise and T. Hanrath, *Nano Letts.* **9** , 3749 (2009).

17. J. M. Luther, M. Law, M. C. Beard, Q. Song, M. O. Reese, R. J. Ellingson and A. J. Nozik, *Nano Letts.* **8** , 3488 (2008).

18. E. H. Sargent, *Nat. Photonics,* **3** , 325 (2009).

19. G. I. Koleilat, L. Levina, H. Shukla, S. H. Myrskog, S. Hinds, A. G. Pattantyus-Abraham and E. H. Sargent, *ACS Nano,* **2** , 833 (2008).

20. N. Zhao, T. P. Osedach, L. Y. Chang, S. M. Geyer, D. Wanger, M. T. Binda, A. C. Arango, M. G. Bawendi and V. Bulovic, *Am. Chem. Soc.* **4,** 3743 (2010).

21. K. W. Johnston, A. G. Pattantyus-Abraham, J. P. Clifford, S. H. Myrskog, D. D. MacNeil, L. Levinaa and E. H. Sargent, *Appl. Phys. Letts.* **92** 151115 (2008).

22. J. Tang, X. Wang, L. Brzozowski, D. Aaron, R. Barkhouse, R. Debnath, L. Levina, and E. H. Sargent, *Adv. Mater.* **22** , 1398 (2010).

23. I. Moreels, K. Lambert, D. De Muynck, F. Vanhaecke, D. Poelman, J. C. Martins, G. Allan, and Z. Hens, *Chem. Mater.* **19,** 6101 (2007).

24. M. Law, J. M. Luther, O. Song, B. K. Hughes, C. L. Perkins and A. J. Nozik, *ACS Nano* **2** , 271 (2008).

25. M. Law, J. M. Luther, O. Song, B. K. Hughes, C. L. Perkins and A. J. Nozik, *J. Am. Chem. Soc.* **130** , 5974 (2008).

26. J. G. R. Briggs, *Science in Focus, Chemistry for GCE'O' Level* (Pearson Education, New Jersey), p. 172 (2005).